

Shearing response of ice-rich rock glacier material

L.U. Arenson, N. Almasi & S.M. Springman

Institute for Geotechnical Engineering, Swiss Federal Institute of Technology, Zurich, Switzerland

ABSTRACT: A series of 10 nominally undisturbed cores from the Murtèl-Corvatsch rock glacier and 2 artificially frozen samples were tested in a triaxial test apparatus at about -2°C to establish shear strength, mobilised as a function of shearing rate, cell pressure and axial strain. These samples varied naturally in content, however, a marked percentage of air (4 – 32%) was present within a matrix of mainly ice, with some solids (0 – 28%). This influenced the volumetric response, which showed a loss of 8 – 10% after 15 – 25% axial strain. The stress-strain response was best represented by a hyperbola, although incorporating an unload (relaxation) reload loop into the stress history caused the maximum shear strength mobilised to rise above the curve predicted from the earlier behaviour. The strength at large strain, however, was not affected by the relaxation. This indicates a temporary healing and stiffening mechanism, which was eliminated again after further shearing.

1 INTRODUCTION

The first deep borehole within Alpine permafrost was drilled in 1987 in the Murtèl-Corvatsch rock glacier, which is located in the Engadin, Swiss Alps. Temperature and deformation monitoring, geophysical investigations, dating of moss, chemical and air bubble analyses as well as analyses of the ice crystals were conducted (e.g. Haeberli et al. 1988, 1997, 1998, 1999, Haeberli 1990, Vonder Mùhll & Haeberli 1990, Vonder Mùhll 1992, Vonder Mùhll & Klingelè 1994, Vonder Mùhll et al. 1998, Lehmann & Green 2000, Arenson et al. 2002). However, no mechanical testing was performed on the cores won from borehole 2/1987.

Several triaxial compression tests were carried out in summer 2001, with cores that were still available. These had been stored in a freezer, in the original plastic liner from the triple-tube drilling, at about -18°C during the subsequent 13 years. The main goal of the study presented within this paper, was the determination of shear strength properties of ice-rich permafrost and the corresponding volumetric strain $\Delta V/V_0$, as well as the pore pressure response during compression. These tests are part of a larger study on the mechanical behaviour of rock glacier material (Arenson 2002), focussing mainly on the deformation behaviour with time under constant loads, i.e. creep, to judge the stability of ice rich Alpine permafrost. The conditions in this series of tests were varied according to the

confining pressure σ_3 , axial strain rate $\dot{\epsilon}_a$, relaxation time, as well as natural variation in sample content.

In contrast to several other investigations on the strength of ice (e.g. Mellor & Cole 1982, Kalifa et al. 1992, Rist & Murrell 1994) or frozen soils (e.g. Jones & Parameswaran 1983, Ting et al. 1983, Andersen et al. 1995), the material under investigation had been obtained from active rock glacier permafrost and the volumetric air content was significantly higher.

Due to a restricted number of cores available for triaxial testing, the amount of test data was rather limited and parameters cannot be given with high confidence levels. However, many interesting trends could be established, which should assist planning for future test programmes and numerical investigations.

2 MATERIAL AND METHODS

A triaxial test device, that had been developed and constructed at the Institute for Geotechnical Engineering at the Swiss Federal Institute of Technology, Zurich, was used for all tests. The apparatus was placed in a cold chamber where the temperature T could be maintained at the desired level ($\pm 1^{\circ}\text{C}$). Due to the large volume of the cell liquid (~ 52 litres), the temperature in the sample could be maintained accurately to within $\pm 0.05^{\circ}\text{C}$.

The triaxial apparatus (Fig. 1) consists of a cell pressure unit with a step motor (1), shaft coupling (2) and a lead screw (3) that controls the volume of the cell pressure cylinder (4), and therefore the pressure in the cell (10), by moving a loading frame (5) up and down. The sample (9), is placed between two platens (6, 7) and is sealed with a rubber membrane and two O-rings against the anti-freeze that was used as cell liquid, which is pressurised to apply the confining pressure σ_3 . The load cell (8) measures the deviator force and is situated just above the top load platen. Both platens may be set up to allow pore-water or pore-air to leave the sample or to measure pore pressures. Counterweights (11) are placed within the legs of the apparatus to balance the weight of the cell.

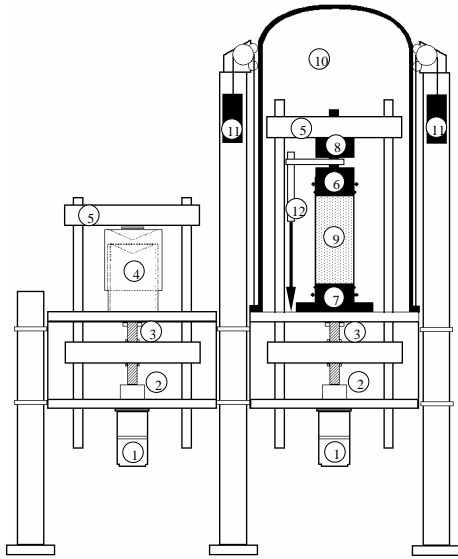


Figure 1. Mechanical set up of the triaxial test apparatus.

Since large strain tests were performed, deformation measurement devices fixed directly to the sample were not considered to be necessary. Therefore, axial deformations were recorded with a displacement transducer (12) fixed between the top platen and the load cell. Volumetric strain ($\Delta V/V_0$) could be determined from measurement of volumetric change in the cell liquid ΔV . Since the sample volume is only about 1.3% of the cell liquid, the accuracy of this measurement is not very good. Nevertheless, trends could be observed after correcting the measured values for changes in temperature.

The samples varied in volumetric ice and air content A_r , as well as in the percentage of solid particles. An overview of the depth and composition of the samples is given in Table 1 together with the applied σ_3 , axial deformation rate and temperature. An increase of solid particles and a decrease of air can be observed with depth. The sample for test No. 9, however, had a stone with a diameter of more than 85 mm that added about 20% to the sample volume. Since the stone was

tilted and was located in the middle of the sample, primarily the shear resistance between the ice and that particular stone was measured.

Table 1. Sample overview.

Test No.	Depth	σ_3	$\dot{\epsilon}_a$	T	Soil composition		
	[m]	[kPa]	[mm/h]	[°C]	Ice / Solids / Air [Vol.-%]		
1	12.0	90.6	40	-2.84	75.2	0.4	24.4
2	10.1	100.7	3.33	-2.08	80.3	0.7	19.0
3	9.9	100.7	10	-2.12	75.3	0.0	24.7
4	7.3	100.8	5	-2.04	67.8	0.0	32.2
5	24.9	180.9	3.33	-2.07	82.3	2.2	15.5
6	25.7	200.7	3.33	-1.96	79.0	6.4	14.6
7	12.5	100.7	10	-1.87	89.5	0.0	10.5
8	15.6	200.7	10	-1.81	81.3	4.7	14.0
9	25.1	180.7	3.33	-1.94	67.5	28.6	3.9
10	4.5	194.1	10	-1.95	69.9	0.2	29.9
11	-	9.0	10	-1.61	96.1	-	3.9
12	-	9.6	10	-1.74	97.7	-	2.3

Two artificially prepared samples were also tested in order to compare the results of the original samples. One sample had been prepared with crushed ice (cru: No. 11, e.g. Jones & Parameswaran 1983, Singh & Jordaan 1996), while water was frozen from the top to the bottom for the other sample to produce columnar-grained ice (col: No. 12).

Before the 75 mm diameter samples were tested, they were cut with a circular saw to the correct length (about 150 mm) and brought to the test temperature by storing them within the plastic liner in the cold room for at least a week. The plastic liner was removed just before the sample was put into the triaxial apparatus using a special template.

All tests were carried out at a temperature of about -2°C , which is similar to what that had been recorded for the Murtèl-Corvatsch rock glacier at a depth of between 12 and 16 m (Vonder Mühl & Haeberli 1990).

3 RESULTS

Initially, all tests were planned to be carried out under undrained conditions, i.e. pore pressures that occurred within the samples could not be dissipated (Fig. 2). The high pore pressures that were measured at the top and the bottom platen indicated that the sample was statically compacted during the shearing due to the compressibility of the air and hence the volume of the sample changed even under undrained conditions. It must also be assumed that air pressures within some closed voids might even be higher than the pressure in the open void system that was measured during the test.

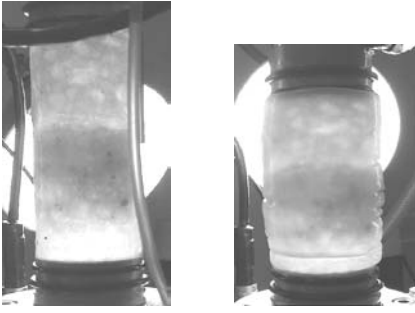


Figure 2. Test No. 2 before (left) and after (right) shearing. Air had accumulated around the sample after shearing.

Four subsequent tests were drained and pore pressures were measured while being allowed to dissipate through the top platen.

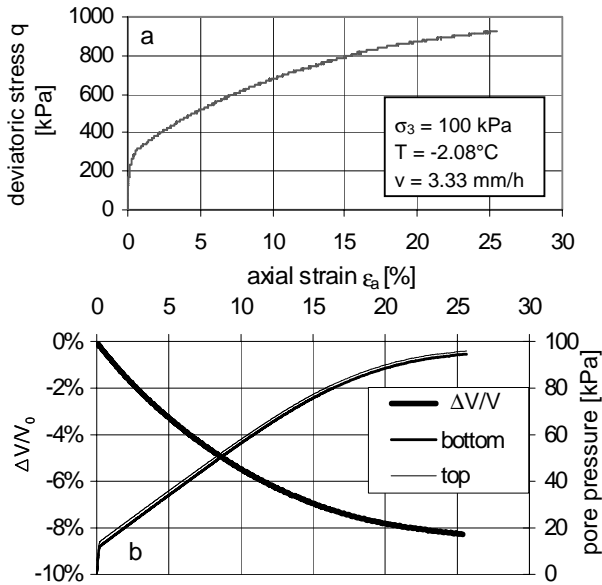


Figure 3. Results of test No. 2, 10 m depth: q (a), $\Delta V/V_0$ and pore pressure (b) versus ϵ_a .

The deviatoric stress ($q = \sigma_1 - \sigma_3$), volumetric behaviour $\Delta V/V_0$ and pore pressures u are plotted versus axial strain ϵ_a for test No. 2 (Fig. 2) and are representative for most of the tests (Fig. 3). Typically, there was a steep increase in resistance for strains smaller than about 1%, followed by yield and strain hardening for the rest of the shearing. The q value of this first ‘plateau’, also referred to as an upper yield region (e.g. Andersen et al. 1995), differed for various deformation rates and sample compositions between 100 kPa and 600 kPa. Usually, the strain hardening lasted until the end of the test, which was set at axial strains between 25 and 35%. The strain hardening was accompanied by a decrease in volume, and this had not reached a constant value by the end of the test, even though volume decreases of up to 10% were registered. Strictly, the measured resistance is not a steady state (critical) value, since the volume had not reached a constant value for most of the tests.

However, the critical state concept may be less useful for frozen soil (Yasufuku et al. 2003) and further shearing would not give any useful results, since boundary effects, such as the friction of the platens or large deformations of the rubber membrane would have influenced the test results (e.g. Head 1996).

The pore pressures shown in Figure 3b also show characteristic behaviour for nearly all of the undrained tests. A steep increase at small strains corresponding to the sharp rise in q (here $\sim 5\%$ q) was followed by a nearly linear increase until more than 10% axial strain. Afterwards, the pore pressures approach the value of σ_3 . The final values of the pore pressures were in a range between 53% and 95% of the applied cell pressure.

In contrast to the undrained tests, drained tests showed a slightly different volumetric behaviour. Test No. 7, however, was the only test that showed dilatancy, i.e. after a volume decrease up to $\epsilon_a \approx 2\%$, the volume started to increase again, at the point where the first peak was achieved in q (Fig. 4). After a relaxation period, the sample was sheared further and $\Delta V/V_0$ remained constant at $+0.2\%$ for $\epsilon_a > 15\%$.

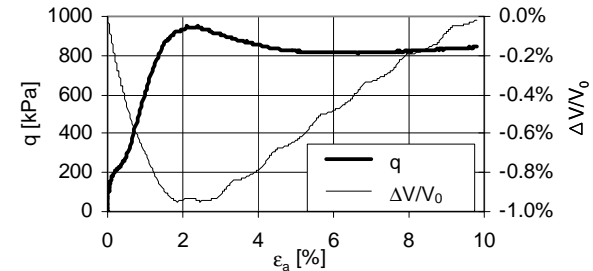


Figure 4. q and $\Delta V/V_0$ for $\epsilon_a < 10\%$ for test No. 7 (drained).

Several tests were stopped with $\epsilon_a > 10\%$, re-shearing commenced following a relaxation of some hours (Fig. 5). Self-healing, which leads even to stronger bonds between the granules of ice and the soil within the crystalline structure, could be assumed based on the increase in the shear resistance upon reloading. Strain softening followed, approaching values of resistance that would probably have been reached without a relaxation. It must be assumed that longer relaxation times might have caused larger peak values since more bonds could refreeze and have to be re-broken. The volume changes, however, seem not to be affected by the relaxation indicating that only the shear zone is affected during the reload, by re-breaking of new bonds between the ice crystals.

A summary of the most important values for all tests is given in Table 2 together with the various different test conditions. Several different shear responses were obtained. Some of the samples showed primarily strain hardening (e.g. Fig. 4) and only when a relaxation was applied, could a peak value be observed (peak 2 in Table 2).

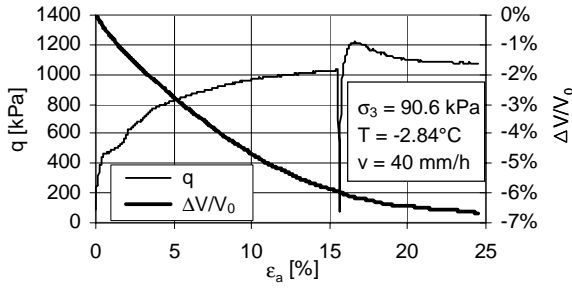


Figure 5. Test No. 1, 12 m depth: deviatoric stress and volume changes against axial strain.

An initial Young's modulus E_{init} and Young's modulus after the relaxation E_{reload} were determined even though the behaviour is highly non-elastic. The moduli were calculated as secant moduli, using $\epsilon_a = 0.2\%$. Generally, the moduli increase with increasing $\dot{\epsilon}_a$ and decrease with increasing A_r .

The two artificially frozen samples (Nos. 11 & 12) contained the least air and mobilised much higher shear strength than the other tests, with a brittle response at $\epsilon_a < 1\%$, without a plateau. Rapid strain softening followed this first peak. In addition, volume increase and negative pore pressures were measured. This is typical for brittle failure, where the whole structure collapses immediately and various pieces of the densely packed sample dilate. The volume of the sample increases, as the pressure in the air decreases. This behaviour was much more pronounced for the columnar grain ice sample.

4 DISCUSSION

The results showed that depending on the applied $\dot{\epsilon}_a$, σ_3 and composition, a whole range of shear responses could be obtained. Consequently, it is not possible to determine unique soil parameters for a rock glacier soil from the test performed within this study. An increase of q can be determined with decreasing A_r and increasing σ_3 (Fig. 6).

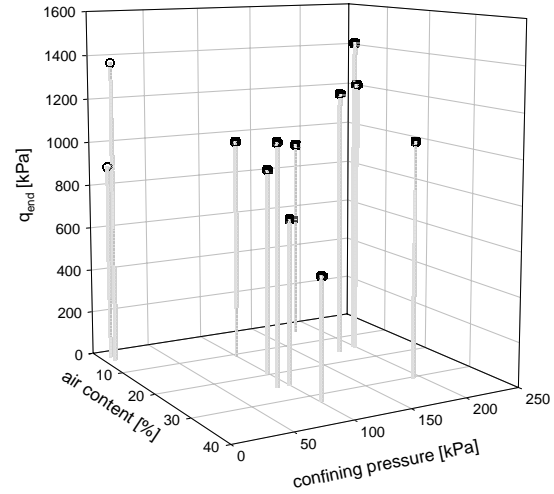


Figure 6. Deviatoric stress at the end of each test as a function of σ_3 and A_r (o: artificial samples).

At the ice content tested (67 – 98%), A_r has a much more important influence than the actual ice content. Various other authors have noted that volumetric ice contents larger than 60% only slightly

Table 2. Summary table of soil properties.

Test ¹	ice	air	σ_3	$\dot{\epsilon}_a$	end			Vol. ⁴	u ⁵	plateau		peak 1 ⁶		peak 2 ⁷		E_{init} ⁸	E_{reload} ⁹	T
					q_{end}	$\epsilon_{a,end}$ ²	$\epsilon_{v,end}$ ³			q	ϵ_a	q	ϵ_a	q	ϵ_a			
	[Vol-%]	[Vol-%]	[kPa]	[s ⁻¹]	[kPa]	[%]	[%]	[kPa]	[kPa]	[kPa]	[%]	[kPa]	[%]	[kPa]	[%]	[GPa]	[GPa]	[°C]
1u	75.2	24.5	90.6	$7.1 \cdot 10^{-5}$	1076	25.3	6.5	nearly	77.9	470	0.62	-	-	1217	16.6	0.18	0.48	-2.84
2u	80.3	19.1	100.7	$5.9 \cdot 10^{-6}$	925	25.4	8.3	nearly	95.3	279	0.37	-	-	-	-	0.18	-	-2.08
3u	75.3	24.7	100.7	$1.9 \cdot 10^{-5}$	738	27.2	8.9	no	82.2	254	0.17	-	-	687	17.4	0.18	0.27	-2.12
4u	67.8	32.2	100.8	$8.6 \cdot 10^{-6}$	544	16.2	9.2	nearly	51.8	180	0.09	-	-	553	13.1	0.10	0.20	-2.04
5u	82.3	15.5	180.8	$6.1 \cdot 10^{-6}$	1224	39.1	9.7	no	164.0	262	0.35	-	-	-	-	0.22	-	-2.07
6u	79.0	14.6	200.7	$6.4 \cdot 10^{-6}$	1258	36.4	10.1	no	129.8	-	-	-	-	-	0.09	-	-1.96	
7d	89.5	10.5	100.7	$1.8 \cdot 10^{-5}$	1014	19.3	-0.2	yes	-0.8	201	0.19	949	2.38	1108	11.7	0.13	0.45	-1.87
8d	81.3	14.0	200.7	$1.8 \cdot 10^{-5}$	1450	24.7	7.8	no	-0.8	610	0.42	-	-	1607	14.8	0.38	0.59	-1.81
9d	67.5	3.9	180.7	$6.2 \cdot 10^{-6}$	938	26.1	1.8	yes	-10.9	-	-	1098	2.93	1109	14.0	0.29	0.48	-1.94
10d	69.9	29.9	194.1	$1.9 \cdot 10^{-5}$	1062	26.7	10.7	no	-0.5	-	-	-	-	1122	16.0	0.21	0.34	-1.95
11u	96.1	3.9	9.5	$1.8 \cdot 10^{-5}$	1380	25.5	-1.7	nearly	-13.4	-	-	2047	0.90	1848	13.2	0.52	0.93	-1.61
12u	97.7	2.3	9.5	$1.8 \cdot 10^{-5}$	896	24.9	-8.9	no	-62.5	-	-	2353	1.06	1285	13.1	0.14	0.77	-1.74

¹ u: undrained test; d: drained test; i.e. the air was allowed to exit through the base platen

² axial strain at the end of a test

³ $\Delta V/V_0$ at the end of a test: negative values indicate a volume increase of the sample

⁴ this column indicates if the volume has reached a constant value at the end of a test or not

⁵ average of pore pressure value measured at the top and the base

^{6,7} peak value with subsequent strain softening before/after the relaxation

^{8,9} Young's modulus at the beginning/for reloading after relaxation: secant module for 0.2% axial strain

influence the strength of frozen soils (e.g. Ting et al 1983). Consequently, tests with similar A_r and $\dot{\epsilon}_a$ were compared and shear parameters could be calculated using a Mohr Coulomb (effective stress) failure criterion, since the pore/air pressures were known. For tests Nos. 2,5 and 6, with A_r between 14 and 19% and $\dot{\epsilon}_a \sim 6 \cdot 10^{-6} \text{ s}^{-1}$, an angle of friction ϕ' of 47.9° and a cohesion c' of 245 kPa were determined. For the second group of tests (Nos. 3 & 10) with A_r of 25% and 29%, and $\dot{\epsilon}_a \sim 2 \cdot 10^{-5} \text{ s}^{-1}$: $\phi' = 28.6^\circ$ and $c' = 248 \text{ kPa}$.

The cohesion c' is due to the strength of the ice and is independent of A_r . The air seems to be predominant, since the applied $\dot{\epsilon}_a$ should have an influence on the shear response (e.g. Rist & Murrell 1994). The difference in the angle of friction ϕ' is mainly due to A_r , which was shown also by Gagnon & Gammon (1995). For higher A_r , dilation is suppressed leading to lower (steady state) friction angles.

The plateau in the q - ϵ diagrams, or first resistance peak for small strains, has also been recorded by several other authors (e.g. Sayles 1974, Mellor & Cole 1982, Jones & Parameswaran 1983, Da Re 2000). In addition, Andersen et al. (1995), who investigated small-strain behaviour for frozen sand, confirmed that the ice matrix, $\dot{\epsilon}_a$ and T dominate the upper yield behaviour, which, however, is still poorly understood.

Comparison between test No. 1 and the two artificially frozen samples showed that brittle failure is not just a function of the axial strain rate (e.g. Kalifa et al. 1992), but also of the air content. Test No. 1 ($A_r = 24.5\%$, $\dot{\epsilon}_a = 7.1 \cdot 10^{-5} \text{ s}^{-1}$) showed a ductile response, whereas the others were brittle, even though $\dot{\epsilon}_a$ was more than three times lower.

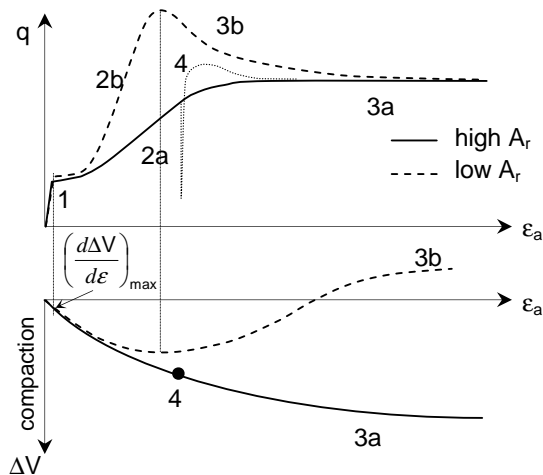


Figure 7. Summary of shear and volumetric response of ice rich soils with large and low air content A_r .

The response of the samples under triaxial compression can be divided into different stages and mechanisms respectively (Fig. 7). An initial breakage of bonds between ice granules is accompanied

by release of air, resulting in a volume decrease (1), which is independent of A_r . For soil with high A_r , the expulsion and compression of the pore air continues together with a rearrangement of the granular ice and soil particles (2a). At large strain, the air is either all dissipated or compressed, allowing only a limited increase in q to be mobilised together with limited further volume change (3a). A relaxation (4) would result in an increase of q due to re-breaking of the re-formed bonds, without affecting the volumetric response. A soil with low A_r is able to mobilise peak strength (2b) until enough air is dissipated so that dilatancy between the ice granules and soil can occur. Typically, this accompanies a volume increase that might even result in a net increase of the sample volume (3b).

The strain hardening, that was recorded for most of the tests on original permafrost samples, could be modelled with a hyperbolic law, ignoring the peak strength behaviour after a relaxation:

$$q = \frac{\epsilon_a}{\frac{1}{E_{init}} + \frac{\epsilon_a}{q_{end}}} \quad (1)$$

E_{init} : initial Young's modulus

q_{end} : shear resistance at large strain

The values for E_{init} and q_{end} are given in Table 2, however, it was not possible to model the volumetric response similarly.

In addition, unfrozen water might also influence the behaviour of the soil close to the melting point (Williams 1967). Since the tests have only been performed at one particular temperature, this effect cannot be quantified, but should be taken into consideration for further investigations.

5 SUMMARY AND CONCLUSIONS

Several triaxial shear tests were performed on samples obtained from a borehole in an Alpine rock glacier. Due to the limited number of successful tests and the heterogeneity of the samples in terms of air content and solids, it was not possible to determine unique frozen soil properties. However, many effects were recognised that are important for the mechanical modelling of rock glacier behaviour and future investigations:

- generally, the material studied contained 10–25% air and was strain hardening under triaxial compression following a hyperbolic q - ϵ_a law, which can be explained by compressibility and expulsion of air,
- volume change is likely to occur under compression, resulting in high air pressures and therefore low effective stresses,
- the shear response is strongly dependent on the volumetric air content,

- failure surfaces have a pronounced self-healing potential following a stress relaxation,
- higher shear stress is required to re-break the newly (re-)formed bonds on a shear surface,
- dilation is only observed for samples with less than 10% air voids, where granules of ice shear past and ride over each other causing volumetric increase,
- it is questionable if steady state (critical) strength will be reached under triaxial compression for $A_r > 10\%$.

Further investigations are clearly necessary, focusing on the effect of cavity air and the granular nature of some rock glacier ice. Since drilling of rock glacier samples is not a simple task, laboratory made samples should be tested in the future. However, they have to be prepared in a way that air is trapped within the sample under comparable conditions. Otherwise, much higher strength values must be expected since the mechanisms change. Furthermore, temperature variations might help in understanding the effect of unfrozen water within the ice matrix.

ACKNOWLEDGEMENT

The authors wish to thank the Department of Geography at the University of Zurich (Prof. W. Haerberli) and the Glaciological Section of the Institute of Hydraulics, Hydrology and Glaciology of ETH (Dr. D. Vonder Muehll) for their trust in handing over the very valuable samples from the drilling programme in 1987. We also acknowledge gratefully the invaluable contributions of Ernst Bleiker and Adrian Zweidler and the workshop with the design, construction and programming of the triaxial test apparatuses, and Marco Sperl with the laboratory testing. The triaxial apparatuses were part-funded by a R'EQUIP grant from the Swiss National Science Foundation. The first author is supported by ETH Research Funds.

REFERENCES

Andersen, G.R., Swan, C.W., Ladd, C.C. & Germain, J.T. 1995. Small-strain behavior of frozen sand in triaxial compression. *Canadian Geotech. J.* 32: 428-451.

Arenson, L.U. 2002. Unstable Alpine permafrost: a potentially important natural hazard – Variations of geotechnical behaviour with time and temperature. *PhD No 14801, Inst. for Geotech. Engng., ETH, Zurich.*

Arenson, L.U., Hoelzle, M. & Springman, S.M. 2002. Borehole deformation measurements and internal structure of some rock glaciers in Switzerland. *Permafrost & Periglacial Proc.* 13: 117-135.

Da Re, G. 2000. Physical mechanisms controlling the pre-failure stress-strain behavior of frozen sand. *PhD, Dept. of Civil & Env. Eng., MIT, Cambridge.*

Gagnon, R.E. & Gammon, P.H. 1995. Triaxial experiments on iceberg and glacier ice. *J. of Glac.* 41: 528-540.

Haerberli, W. (ed.) 1990. Pilot analyses of permafrost cores from the active rock glacier Murtel I, Piz Corvatsch, Eastern Swiss Alps. *A Workshop Report.*

Haerberli, W., Huder, J. & Keusen, H.R. 1988. Core drilling through rock glacier permafrost. *Proc. 5th Int. Conf. on Permafrost, Trondheim:* 937-942.

Haerberli, W., Wegmann, M. & Vonder Muehll, D. 1997. Slope stability problems related to glacier shrinkage and permafrost degradation in the Alps. *Eclogae Geologicae Helveticae* 90: 407-414.

Haerberli, W., Hoelzle, M., Käab, A., Keller, F., Vonder Muehll, D. & Wagner, S. 1998. Ten years after drilling through the permafrost of the active rock glacier Murtel, eastern Swiss Alps: Answered questions and new perspectives. *Proc. 7th Int. Conf. on Permafrost, Yellowknife:* 403-410.

Haerberli, W., Käab, A., Wagner, S., Vonder Muehll, D., Geissler, P., Haas, J.N., Glatzel-Mattheier, H. & Wagenbach, D. 1999. Pollen analysis and ¹⁴C age of moss remains in permafrost core recovered from the active rock glacier Murtel-Corvatsch, Swiss Alps: geomorphological and glaciological implications. *J. of Glac.* 45: 1-8.

Head, K.H. 1996. *Manual of soil laboratory testing, Vol. 3: Effective Stress Tests.* West Sussex: John Wiley & Sons.

Jones, S.J. & Parameswaran, V.R. 1983. Deformation behavior of frozen sand-ice materials under triaxial compression. *Proc. 4th Int. Conf. on Permafrost, Fairbanks:* 560-565.

Kalifa, P., Ouillon, G. & Duval, P. 1992. Microcracking and failure of polycrystalline ice under triaxial compression. *J. of Glac.* 38: 65-76.

Lehmann, F. & Green, A. 2000. Topographic migration of georadar data: Implications for acquisition and processing. *Geophysics* 64: 836-848.

Mellor, M. & Cole, D.M. 1982. Deformation and failure of ice under constant stress or constant strain-rate. *Cold Regions Science and Technology* 5: 201-219.

Rist, M.A. & Murrell, S.A.F. 1994. Ice triaxial deformation and fracture. *J. of Glac.* 40: 305-318.

Sayles, F.H. 1974. Triaxial constant strain rate tests and triaxial creep tests on frozen Ottawa sand. *CRREL Report* 253.

Singh, S.K. & Jordaan, I.J. 1996. Triaxial tests on crushed ice. *Cold Regions Science and Technology* 24: 153-165.

Ting, J., Martin, T. & Ladd, C. 1983. Mechanisms of strength for frozen sand. *J. of Geotech. Eng.* 109: 1286-1302.

Vonder Muehll, D. 1992. Evidence of intrapermafrost groundwater flow beneath an active rock glacier in the Swiss Alps. *Permafrost & Periglacial Proc.* 3: 169-173.

Vonder Muehll, D. & Haerberli, W. 1990. Thermal characteristics of the permafrost within an active rock glacier (Murtel/Corvatsch, Grisons, Swiss Alps). *J. of Glac.* 36: 151-158.

Vonder Muehll, D. & Klingelé, E. 1994. Gravimetric investigation of ice-rich permafrost within the rock glacier Murtel-Corvatsch (Upper Engadin, Swiss Alps). *Permafrost & Periglacial Proc.* 5: 13-24.

Vonder Muehll, D., Stucki, T. & Haerberli, W. 1998. Borehole temperatures in Alpine permafrost: a ten year series. *Proc. 7th Int. Conf. on Permafrost, Yellowknife:* 1089-1095.

Williams, P.J. 1967. Unfrozen water content of frozen soils and soil moisture suction. *Norwegian Geotech. Inst.* 72: 11-26.

Yasufuku, N., Springman, S.M., Arenson, L.U. & Ramholt, T. 2003. Stress-dilatancy behaviour of frozen sand in direct shear. *Proc. 8th Int. Conf. on Permafrost, Zurich:* current issue.